Available online at www.sciencedirect.com
SCIENCE DIRECT®
Coordination Chemistry Reviews 248 (2004) 1447–1453
COORDINATION CHEMISTRY REVIEWS
www.elsevier.com/locate/ccr

Review

Electrochemical studies of the Co(III)/Co(II)(dbbip)$_2$ redox couple as a mediator for dye-sensitized nanocrystalline solar cells

Petra J. Cameron [a], Laurence M. Peter [a,*], Shaik M. Zakeeruddin [b], Michael Grätzel [b]

[a] *Department of Chemistry, University of Bath, Bath BA2 7AY, UK*
[b] *Laboratory for Photonics and Interfaces, Swiss Federal Institute of Technology, CH-1055 Lausanne, Switzerland*

Received 31 October 2003; accepted 9 February 2004
Available online 9 April 2004

Contents

Abstract

The electrochemical properties of the redox mediator Co(III)/Co(II)(dbbip)$_2$ (dbbip = 2,6-bis(1′-butylbenzimidazol-2′-yl)pyridine) in a mixed acetonitrile/ethylene carbonate solvent have been studied by a range of techniques in order to determine the rate constants for electron transfer and the diffusion coefficients of the Co(II) and Co(III) species. Platinum, gold, fluorine-doped tin oxide (FTO) and compact TiO_2 layers were used as electrode materials. The results have been used to predict the limitations imposed on the performance of dye-sensitized nanocrystalline cells by the electron transfer kinetics and mass transport properties of the redox mediator. The Co(III)/Co(II) redox mediator is compared with the conventional triiodide/iodide redox system used in high performance dye-sensitized solar cells.

Keywords: Cobalt; Dye-sensitized; Solar cell; Titanium dioxide

1. Introduction

The dye-sensitized nanocrystalline solar cells pioneered by Grätzel and co-workers [1–6] rely on a liquid redox electrolyte (also known as a supersensitizer) to regenerate the light-harvesting dye following the photoinduced charge injection step. In spite of efforts to optimize the cells and to develop alternative charge transport and regeneration systems such as organic [7,8] or inorganic [9–13] hole conductors, the best efficiencies have been obtained using the triiodide/iodide redox couple in a liquid electrolyte [14]. One-electron outer sphere redox systems with rapid electron exchange kinetics such as ferrocene/ferricinium give low photovoltages and low photocurrents as a consequence of rapid back reaction of photoinjected electrons with the oxidized redox component [15]. The reason that the triiodide/iodide system works so well appears to be that the transfer of electrons from the TiO_2 to I_3^- ions in the electrolyte is a slow two-electron transfer process. In contrast, regeneration of I^- from I_3^- at the platinum counter-electrode is very rapid as a consequence of electrocatalysis via dissociative chemisorption of I_2. In addition, the strong adsorption of iodide and triiodide ions on platinum should provide protection against the effects of electrode contamination on the rate of regeneration. This contrasts with the case of uncatalyzed electrode processes, such as those involving outer sphere electron transfer reactions on metal electrodes, where the rate constants for electron transfer may be lowered by orders of magnitude by adsorption of impurities.

A successful redox mediator must exhibit fast electron transfer kinetics at the metal counter electrode in order to minimize voltage losses, but it must also display slow elec-

* Corresponding author.
E-mail address: l.m.peter@bath.ac.uk (L.M. Peter).

0010-8545/$ – see front matter © 2004 Elsevier B.V. All rights reserved.
doi:10.1016/j.ccr.2004.02.010

tron transfer kinetics at TiO_2 in order to prevent loss of photoinjected electrons by transfer to the oxidized component of the couple. Several cobalt complexes have been suggested as candidate materials [16–18], but detailed studies of the kinetics of these systems have not been carried out. The electron transfer kinetics of octahedral Co(III)/Co(II) complexes are expected to be slow if electron transfer is associated with a change in spin multiplicity. In addition, the inner sphere reorganization energy will also be high if, as a consequence, the Co–ligand bond lengths differ in the Co(III) and Co(II) complexes. However, slow electron exchange kinetics is not a sufficient criterion for selecting cobalt systems as redox relays. A key question is whether the cobalt-based redox systems will exhibit fast kinetics at the metal electrode and slow kinetics at the nanocrystalline TiO_2. It is not easy to answer this question a priori, since the states involved in electron transfer are different in the two cases. At a metal electrode, electron exchange with the redox system occurs predominantly at energies close to the Fermi level. In the case of semiconductors like nanocrystalline TiO_2, electrons may be in the conduction band, leading to a highly exoenergetic reaction with the Co(III) species, or they may be located at surface state energy levels in the band gap, in which case the reaction is less exoenergetic. A further complication is that electron transfer to the Co(III) species may occur from the conducting fluorine-doped tin oxide (FTO) substrate, effectively shunting the solar cell. For this reason, we have examined the electron transfer kinetics of the cobalt complex at platinum and gold electrodes as well as at FTO films and TiO_2 blocking layers.

Recently Nusbaumer et al. [17,18] reported cells containing a cobalt-based redox mediator, $Co(II)(dbbip)_2(ClO_4)_2$ (dbbip = 2,6-bis(1′-butylbenzimidazol-2′-yl)pyridine (see Fig. 1 for the structure of the complex) that achieved efficiencies of up to 5.5% at 1/10 sun illumination (AM 1.5). This interesting result stimulated us to perform a detailed electrochemical study of this redox system in order to identify why it works so well compared with other one-electron metal–ligand redox systems such as ferrocene/ferricinium [15]. Electrochemical techniques were used to study the kinetics of electron exchange of $Co(II)(dbbip)_2$ and $Co(III)(dbbip)_2$ at platinum, gold, FTO, platinum-coated FTO and TiO_2-coated FTO. Electron transfer rate constants and diffusion coefficients are reported and used to predict the behavior of the redox system in the thin layer solar cell configuration under operating conditions. The results have revealed that the kinetics of electron transfer in the Co(III)/Co(II) system on metal electrodes are quite slow, so that significant voltage losses at the solar cell counter electrode may be expected unless steps are taken to increase the electrode area. In addition, the diffusion coefficients of the oxidized and reduced species are relatively low, so that mass transport limitations may be a problem. The data reported in this paper illustrate how the results of electrochemical measurements can be used to develop quantitative models of the performance of dye-sensitized nanocrystalline solar cells employing new redox mediators such as $Co(II/II)(dbbip)_2$.

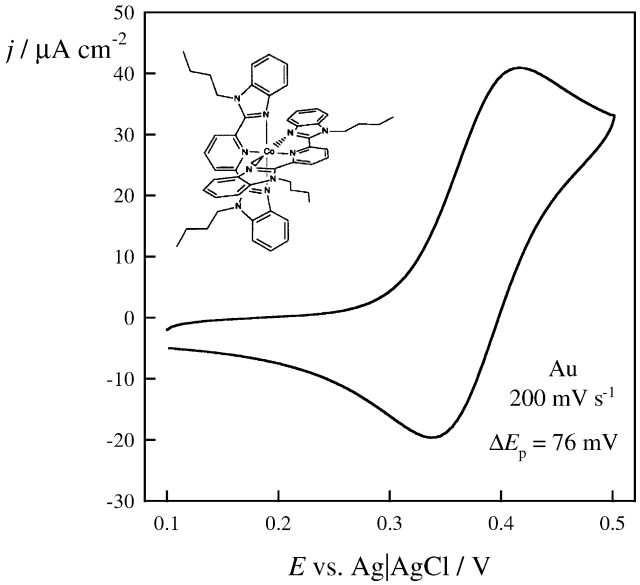

Fig. 1. Cyclic voltammogram showing quasi-reversible behavior of the Co(III)/Co(II)$(dbbip)_2$ system at a gold electrode (ϕ = 125 μm). 1.0×10^{-3} M $Co(dbbip)_2{}^{2+}$ + 0.1 M tetrabutylammonium hexafluorophosphate in ethylene carbonate/acetonitrile (60:40). Sweep rate: 200 mV s^{-1}. The inset shows the structure of the complex.

2. Experimental

Cyclic voltammetry was carried out in a conventional three electrode configuration using a platinum disc working electrode (ϕ = 500 μm) and a gold disc electrode (ϕ = 125 μm) in a de-oxygenated solution consisting of 1 mM $Co(II)(dbbip)_2(ClO_4)_2$ in 60% ethylene carbonate (Aldrich, anhydrous)/40% acetonitrile (Fisher, HPLC grade dried over molecular sieves) with 0.1 M tetrabutylammonium hexafluorophosphate (Aldrich) background electrolyte. In order to prevent contamination of the electrolyte with water and chloride ions, a platinum wire quasi-reference electrode (QRE) was used. At the end of the experimental run, a reference voltammogram was recorded by replacing the QRE with an Ag/AgCl reference electrode, so that the potential scales on the voltammograms could be converted. A platinum foil counter electrode completed the cell. Electrochemical measurements were performed with an Eco Chemie P12 Autolab system under computer control.

Thin layer cells were constructed using Hartford glass (FTO: fluorine doped tin oxide-coated glass, Hartford Glass, USA, sheet resistance: 15 Ω per square). The electrode area was 1 cm^2. The glass was cleaned twice in 5% Deconex for 15 min, rinsed well with Milli-Q water and then consecutively sonicated in isopropanol, ethanol and acetonitrile for 15 min each. Uncoated FTO plates were used directly. Platinum-coated FTO plates were made by sputtering a

thin layer of platinum onto the clean substrate. Compact TiO_2 blocking layers were deposited by spray-pyrolysis using a hand held atomizer, following the method developed by Kavan and Grätzel [19] in which a solution of 0.2 M titanium di-isopropoxide bis(acetylacetonate) (Aldrich) in isopropanol is sprayed in pulses of 1 s duration onto the FTO substrate placed on a hotplate at 450 °C. The thickness of the blocking layers prepared in this way lies in the range 60–120 nm. The counter electrode in the thin layer cells was a FTO glass plate coated with a sputter-deposited layer of platinum. The two electrodes were heat-sealed together with a 50 μm Surlyn® gasket. The cobalt complex electrolyte[1] was a mixture of 0.162 M Co(II)$(dbbip)_2^{2+}$ and 0.018 M Co(III)$(dbbip)_2^{3+}$ in 60% ethylene carbonate/40% acetonitrile. Co(III)$(dbbip)_2^{3+}$ was formed by completely oxidizing a 0.18 M solution of Co(II)$(dbbip)_2^{2+}$ with stoichiometric amounts of $NOBF_4$. The electrolyte was introduced into the cell through holes drilled in the counter electrode, which were subsequently heat-sealed with glass cover slips using Surlyn® film. The final electrode separation in the cells after sealing was 45 μm.

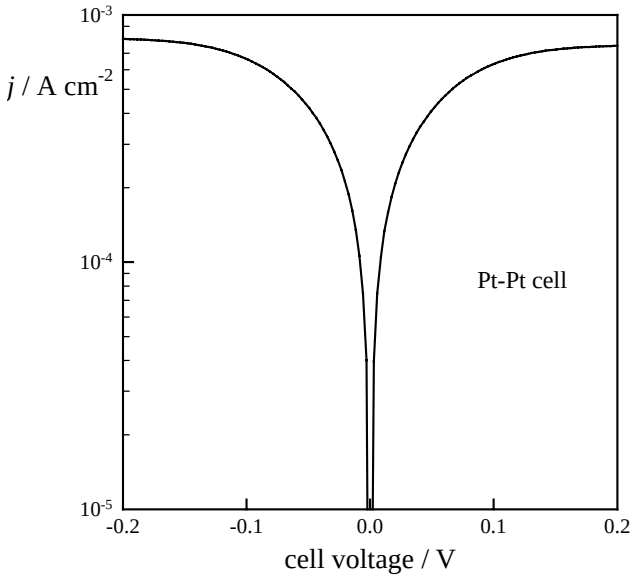

Fig. 2. Current–voltage characteristics of a thin layer cell with sputtered platinum film electrodes. Inter-electrode spacing: 45 μm. Electrolyte: 0.018 M Co(III)$(dbbip)_2$ and 0.162 M Co(II)$(dbbip)_2$.

3. Results and discussion

The electrochemical behavior of Co(II)$(dbbip)_2^{2+}$ was investigated at platinum and gold inlaid disc electrodes. Fig. 1 shows a cyclic voltammogram recorded at a sweep rate of 200 mV s^{-1} at the gold disk electrode. The voltammogram is typical for so-called quasi-reversible behavior associated with rather slow electron transfer kinetics, with a peak separation of 76 mV, rather than the 59 mV expected for the reversible case (fast electron transfer). At the same sweep rate, the peak separation measured using the platinum electrode was 110 mV. The standard reduction potential of the Co(III)/Co(II) system was calculated to be 0.39 V versus Ag/AgCl at both Pt and Ag. Although the system is clearly not completely reversible, inspection of the numerical solution for the current function [20] reveals that the error in using the peak current expression for the reversible case is small in the range of sweep rates used here. Consequently, a plot of the peak current density, $j_{p,\,ox}$ versus the square root of the scan rate can be used to estimate the diffusion coefficient of the Co(II) complex. Plots constructed using data obtained with Pt and Au electrodes both gave a value of 1.9×10^{-6} cm^2 s^{-1} for the diffusion coefficient of the bulky Co(II)$(dbbip)_2^{2+}$ in the mixed solvent (60% ethylene carbonate/40% acetonitrile). This is substantially lower than the value of 7.7×10^{-6} cm^2 s^{-1} given by Nusbaumer et al. [18], who have obtained it for an acetonitrile solution rather than for the more viscous solvent mixture (40:60 acetonitrile/ethylene carbonate) used in the solar cell experiments. Order of magnitude values of the standard rate constant estimated from the peak potential separations in the cyclic voltammograms are 10^{-2} cm s^{-1} for Au and 10^{-3} cm s^{-1} for Pt. The dependence on electrode material may reflect double layer effects or the electronic structure of the electrode. Recent studies of the Co$(phen)_2^{2+/3+}$ system in aqueous supporting electrolytes on single crystal platinum [21] showed that adsorbed anions can influence the rate of electron transfer. These authors reported values of k^0 in the range 0.1 to 10^{-2} cm s^{-1}.

Parallel plate thin layer cells were constructed to investigate the electrode kinetics of the electrolyte (containing both Co(II) and Co(III) forms of the complex) used in dye-sensitized solar cells. The electrode materials investigated were sputtered platinum, FTO, and FTO-coated with a TiO_2 blocking layer. In all cases a platinum-coated FTO counter electrode completed the sandwich cell. Fig. 2 illustrates the current voltage plots for the symmetrical platinum|platinum cell. It can be seen that the current reaches a plateau for small voltages of either polarity. Since the Co(III) species is the minority component, its reduction to Co(II) at the cathode will become mass transport limited when the rate of electron transfer is sufficiently high. Since the concentration gradient across the thin layer cell is linear under stationary conditions and the process is regenerative, calculation of the diffusion coefficient of the Co(III) complex ion using Fick's first law is straightforward.

$$j_{\mathrm{lim,c}} = FD_{\mathrm{Co(III)}} \left.\frac{\mathrm{d}[\mathrm{Co(III)}]}{\mathrm{d}x}\right|_{x=0} = 2FD_{\mathrm{Co(III)}} \frac{[\mathrm{Co(III)}]_{\mathrm{bulk}}}{d} \quad (1)$$

where $j_{\mathrm{lim,\,c}}$ is the limiting cathodic current density, $D_{\mathrm{Co(III)}}$ is the diffusion coefficient of the Co(III) species and d is the

[1] We are grateful to S.M. Zakeeruddin (EPFL) for supplying us with the Co(II)$(dbbip)_2$ complex.

separation between the electrodes (45 μm). The observed limiting current in Fig. 2 gives a value of 1.1×10^{-6} cm^2 s^{-1} for the diffusion coefficient of the Co(III) complex.

Analysis of the current voltage plots obtained in the symmetrical two-electrode thin layer cell configuration is complicated by the fact that there is no reference electrode. At each electrode in the thin layer cell, the current potential relationship is described by the Butler Volmer equation.

$$j = nFk^0[C_R^\sigma \, e^{(1-\alpha)nF(E-E^0)/RT} - C_O^\sigma \, e^{-\alpha nF(E-E^0)/RT}] \quad (2)$$

Here $n = 1$ is the number of electrons transferred, k^0 is the standard heterogeneous rate constant for electron transfer, α is the cathodic transfer coefficient, C_R^σ and C_O^σ are the concentrations of reduced and oxidized cobalt species at the electrode surface, E is the electrode potential and E^0 is the standard electrode potential. Since the concentrations of the Co(II) and Co(III) species at the two electrode surfaces deviate from their bulk values when current flows, the Butler Volmer equation must be reformulated to include the effects of mass transport as follows [20]:

$$\frac{j}{j_0} = \left(1 - \frac{j}{j_{\text{lim,a}}}\right) e^{(1-\alpha)nF\eta/RT} - \left(1 - \frac{j}{j_{\text{lim,c}}}\right) e^{-\alpha nF\eta/RT} \quad (3)$$

Here j_0 is the exchange current density, $nFk^0 C_O^{(1-\alpha)} C_R^\alpha$, $j_{\text{lim, a}}$ and $j_{\text{lim, c}}$ are the anodic and cathodic limiting current densities, respectively, and η is the overpotential $E - E_{\text{eq}}$. The limiting currents that appear in Eq. (3) are determined by Eq. (1) and its analog for the oxidation of Co(II) species, but in practice, the maximum current that can be passed in the thin layer cell will be determined by the minority Co(III) species.

Fig. 3 illustrates the current potential characteristics calculated from Eq. (3) for different values of the standard heterogeneous rate constant k^0. Application of the mass conservation condition in the regenerative thin layer cell restricts the current to the limiting value for reduction of Co(III). It follows that the overpotential at the anode (where oxidation of Co(II) occurs) can be calculated as a function of the current at the cathode using the plot. The highest value of the overpotential at the anode (corresponding to the limiting cell current) varies from 23 to 155 mV as k^0 is decreased from 10^{-3} to 10^{-5} cm s^{-1}.

The total cell voltage, V, is equal to the difference between the anodic and cathodic overpotentials, so that it is possible to compute the j–V characteristics of the cell. A reasonable fit to the experimental j–V plot is obtained for $k^0 = 2.5 \times 10^{-4}$ cm s^{-1} as illustrated in Fig. 4. This is considerably lower than the value of 10^{-2} cm s^{-1} estimated from the cyclic voltammograms recorded for a clean gold disc electrode (cf. Fig. 1). It is also lower than the value of 10^{-3} cm s^{-1} measured using the platinum disk electrode. Sapp et al. [16] have noted that the rate constants for electron exchange of polypyridine complexes of Co(III)/Co(II) are lower at platinum than at gold electrodes. The rea-

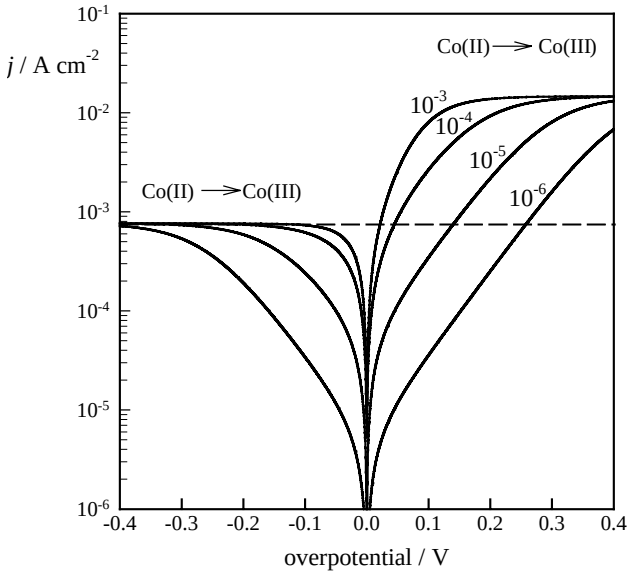

Fig. 3. Current–potential characteristics calculated for a one-electron redox system such as Co(III)/Co(II)(dbbip)$_2$ with mass transport limits determined by an inter-electrode spacing of 45 μm. The diffusion coefficients of the oxidized and reduced components are 1.1×10^{-6} and 1.9×10^{-6} cm^2 s^{-1}, respectively. Concentrations of oxidized and reduced components are 0.018 and 0.162 M. Cathodic transfer coefficient 0.5. Standard heterogeneous rate constant, k^0, as shown. The dashed line shows the mass transport limited current that would be observed in a thin layer cell configuration as a consequence of the fact that the concentration of oxidized species is smaller than that of the reduced species.

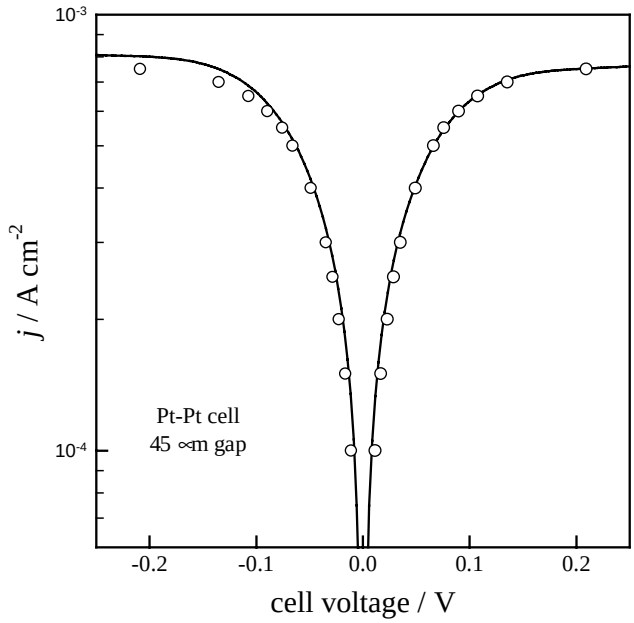

Fig. 4. Comparison of the experimental current–voltage characteristics of the symmetrical Pt–Pt thin layer cell (line) with the current–voltage behavior calculated using the experimental values of the concentrations and diffusion coefficients and a value of the standard heterogeneous rate constant, $k^0 = 2.5 \times 10^{-4}$ cm s^{-1}.

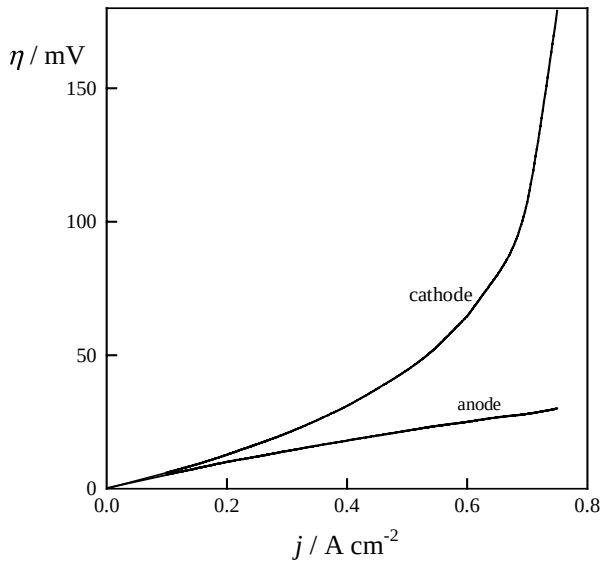

Fig. 5. Calculated anodic and cathodic overpotentials in the Pt–Pt thin layer cell as a function of current density. Note that the overpotential at the cathode increases rapidly as mass transport limitation sets in. By contrast, the smaller overpotential at the anode is determined by the sluggish electron transfer kinetics as well as mass transport.

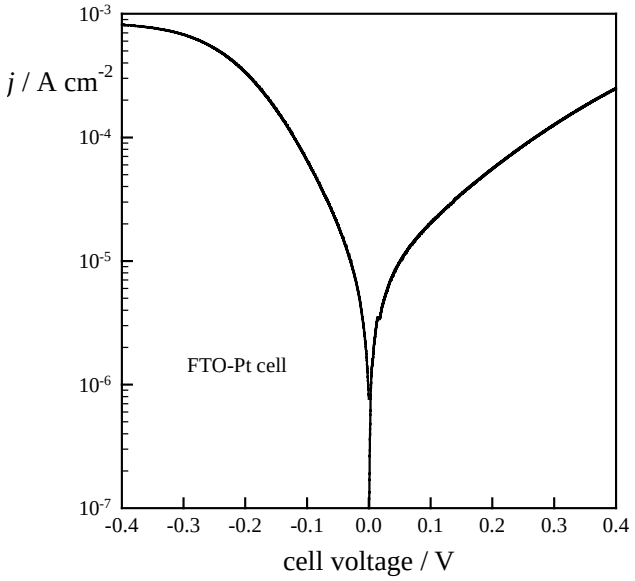

Fig. 6. Current–voltage characteristics of the FTO–Pt cell. Inter-electrode separation 45 μm. The electrolyte is the same as that used in the Pt–Pt cell (Fig. 2). Note that the current only just reaches the mass transport limit at −0.4 V, showing that electron transfer is slower at FTO than at Pt (compare Fig. 2).

sons for the differences in k^0 are not clear, but contamination of the electrode surface could be a contributory factor for an outer sphere electron transfer process as noted earlier.

The low diffusion limited current and the rather small exchange current density for the Co(III)/Co(II) couple at platinum can have important implications for the potential performance of dye-sensitized cells containing the $Co(dbbip)_2$ redox couple. The fit of the current voltage characteristics shown in Fig. 4 was obtained by calculating the contributions from the anode and cathode in the symmetrical thin layer cell. Fig. 5 shows how the overpotentials at the platinum anode and cathode vary with current density for $k^0 = 2.5 \times 10^{-4}\,cm\,s^{-1}$. In the dye-sensitized solar cell, it is the cathode overpotential that is of interest since it represents a voltage loss. Fig. 5 predicts that this loss will increase rapidly when the current density exceeds $0.6\,mA\,cm^{-2}$. It should be possible to reduce this overpotential by increasing the surface roughness of the counter electrode and by replacing platinum with gold or carbon [16], but even if this strategy is successful, the voltage losses may still be a problem at the higher current densities corresponding to 1 sun.

It is clear from the results presented here that a conventional sealed cell with a gap of 45 μm, the low diffusion coefficient of Co(III) complex in the acetonitrile/ethylene carbonate solvent mixture will limit the maximum current to about $1\,mA\,cm^{-2}$. The higher currents reported by Nusbaumer et al. (over $6\,mA\,cm^{-2}$ for 1 sun [17]) were obtained using a 6 μm thick TiO_2 layer with the counter electrode pressed directly on top of the film. It is reasonable to attribute the six-fold higher current observed in this configuration to a reduction of the inter-electrode gap from 45 to around 8 μm. However, the higher current density in this case will lead to a larger overpotential at the platinum counter electrode, and hence an increased voltage loss.

In conventional dye-sensitized solar cells employing the triiodide/iodide redox couple, good performance can be achieved without using a blocking TiO_2 layer to coat the fluorine doped tin oxide prior to deposition of the porous nanocrystalline TiO_2 layer. These cells perform well because the rate of electron transfer from the highly doped n-type SnO_2(F) substrate to I_3^- is a very slow two-electron process [22]. In the case of cells based on the $Co(dbbip)_2$ redox couple, a blocking layer appears to be necessary to prevent the reduction of the Co(III) species at exposed areas of the underlying substrate [17]. This conclusion is confirmed by the current voltage plot obtained using a thin layer cell with a platinum coated electrode paired with an uncoated FTO electrode (Fig. 6).

The asymmetry in the current–voltage characteristics seen in Fig. 6 suggests that the oxidation of Co(II) is less facile than reduction of Co(III) at FTO. The most likely explanation of this is that the latter process involves electron tunneling through the depletion layer formed at the FTO–electrolyte interface. The cathodic process (reduction of the Co(III) complex) is the one that is relevant in the context of the solar cell, since it represents a loss mechanism. In the asymmetric sandwich cell, the overpotential at the platinum electrode is much smaller than at the FTO electrode. Nevertheless, a small correc-

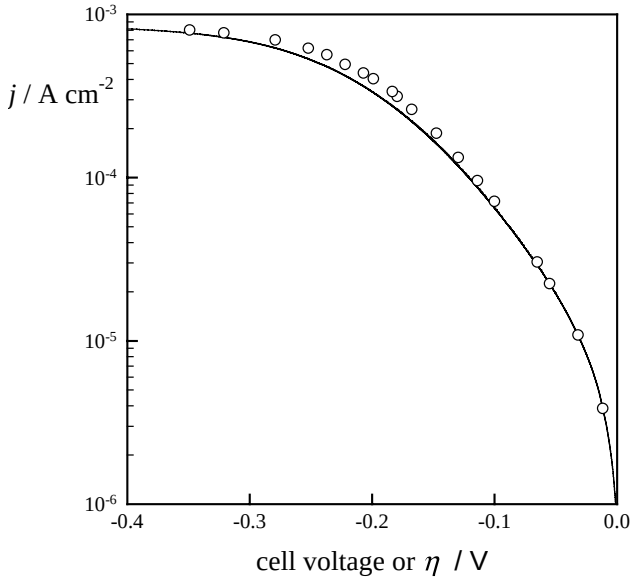

Fig. 7. Comparison of the negative branch of the current–voltage characteristic of the FTO–Pt thin layer cell (line) with the current overpotential characteristic of the FTO electrode calculated by correcting for the overpotential at the Pt anode (open circles). Note that in this case, the anode overpotential is much less than the cathode overpotential, so the correction is small.

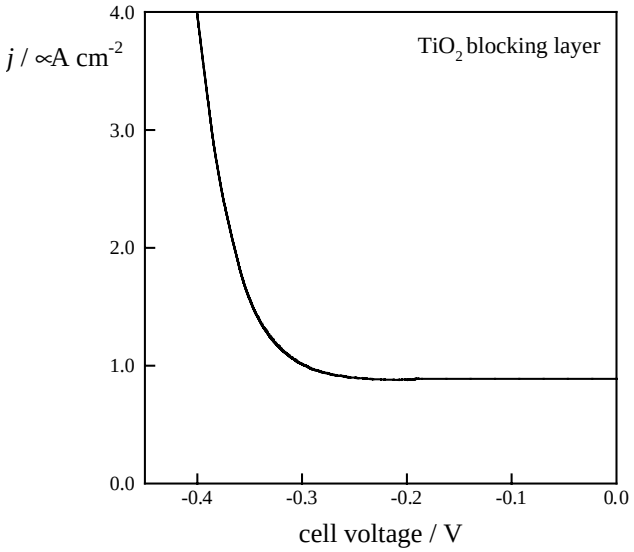

Fig. 9. Current–voltage characteristics of a thin layer cell consisting of a platinum electrode and an electrode fabricated by coating FTO with a thin blocking layer of TiO_2. Inter-electrode separation: 45 μm. Electrolyte as in Pt–Pt cell. Note that the diode characteristics arising from the n-type nature of the blocking layer limit the current for the reduction of $Co(III)(dbbip)_2$ to much lower levels than those observed for uncoated FTO (cf. Fig. 6).

tion for the overpotential at the platinum electrode was made using the value of k^0 determined in the symmetrical cell to give the Tafel plot shown in Fig. 7. Finally the current–overpotential data were corrected for mass transport (cf. Eq. (3)) to give the Tafel plot shown in Fig. 8.

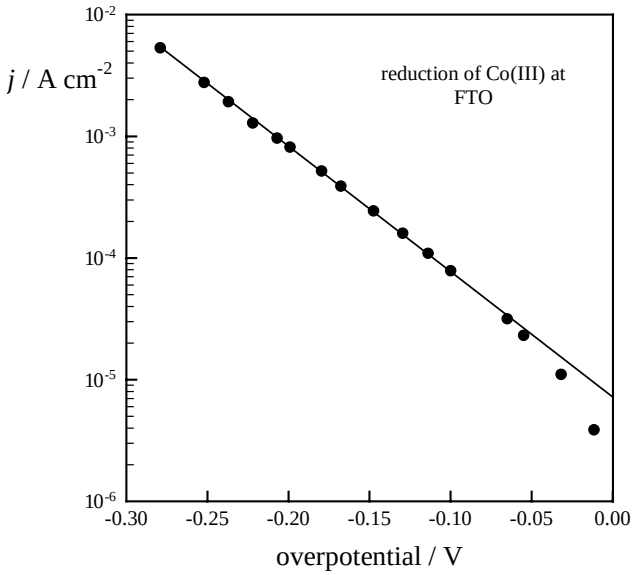

Fig. 8. Tafel plot for the reduction of $Co(III)(dbbip)_2$ at FTO obtained by correcting for the effects of mass transport. The exchange current density obtained from the intercept is 7×10^{-6} A cm^{-2}. This is about 2 orders of magnitude smaller than the value measured for a platinum cathode, but more than 2 orders of magnitude larger than the exchange current density of the I_3^-/I^- redox couple in the same electrolyte. Note the asymmetry in the current voltage characteristics, which is attributed to the fact that FTO is a highly doped n-type semiconductor rather than a metal.

The exchange current density for the Co(III)/Co(II) couple at FTO derived from Fig. 8 is 7×10^{-6} A cm^{-2}, which corresponds to $k^0 = 1.4 \times 10^{-6}$ cm s^{-1}. This is at least 2 orders of magnitude lower than the k^0 value measured for platinum, showing that the nature of the substrate does influence the rate constant for the Co(III)/Co(II) redox couple, in spite of the fact that it is an outer sphere reaction. However, the exchange current density of the Co(III)/Co(II) couple at FTO is more than 2 orders of magnitude higher than that of the I_3^-/I^- couple measured in the same electrolyte ($\approx 10^{-8}$ A cm^{-2}). This explains why a blocking layer is necessary in the solar cell to prevent losses under operating conditions.

A recent study of blocking TiO_2 layers in conventional I_3^-/I^- cells has shown that the films are n-type and exhibit rectifying behavior [22]. This is confirmed by the current voltage characteristics for $Co(III/II)(dbbip)_2^{2+/3+}$ electrolyte at an FTO surface coated with a compact TiO_2 blocking layer. The *j–V* plot is shown in Fig. 9. The effect of the blocking layer is remarkable. It reduces the current flowing at voltages less than −0.3 to around 1 μA cm^{-2}. The diode behavior extends into the anodic branch (not shown). The increase in current at potentials more negative than −0.3 V indicates that the surface density of electrons in the TiO_2 increases as the potential moves toward flatband, but the current is still orders of magnitude smaller than it is on uncoated FTO. Further work is in progress to evaluate the performance of the blocking layers in dye-sensitized solar cells employing the cobalt mediator.

4. Conclusions

The Co(III)/Co(II)(dbbip)$_2$ redox mediator exhibits slow electron exchange kinetics at platinum and fluorine-doped tin oxide electrodes. In spite of the fact that it is an outer sphere redox system, electron exchange is faster at platinum than at FTO. However, the exchange current density at platinum is much smaller than for the I_3^-/I^- system, leading to voltage losses. Strategies to overcome this include increasing the active area of the electrode by nanostructuring and increasing the rate constant for electron transfer by choice of different electrode materials (e.g. gold instead of platinum). The exchange current density for electron transfer at FTO is at least 2 orders of magnitude higher than for the conventional I_3^-/I^- redox mediator, and for this reason it is essential to use a compact TiO_2 blocking layer to prevent efficiency losses due to transfer of electrons from the FTO substrate to the Co(III) species. The diffusion coefficients of the Co(II) and Co(III) species in acetonitrile/ethylene carbonate system are small, so that it is necessary to minimize the electrode spacing to prevent mass transport limitations. The kinetics of electron transfer from nanocrystalline TiO_2 to the Co(III) complex were not addressed in the present study, which used model thin layer systems. Details of the investigation of this process in complete dye-sensitized cells will be given elsewhere [23].

Acknowledgements

This work was supported by the UK Science and Engineering Research Council, Johnson Matthey PLC and by the University of Bath. The authors thank Dr. Shaik M. Zakeeruddin for providing a sample of Co(II)(dbbip)$_2$(ClO$_4$)$_2$. In addition the authors thank Professor Michael Grätzel and Mr. Hervé Nusbaumer (EPFL) for collaboration and helpful discussions. PJC also thanks Mike Cass and Jessica Krüger (EPFL) for assistance.

References

[1] B. O'Regan, M. Grätzel, Nature 353 (1991) 737.
[2] M. Grätzel, Coord. Chem. Rev. 111 (1991) 167.
[3] M. Grätzel, K. Kalyanasundaram, Curr. Sci. 66 (1994) 706.
[4] M. Grätzel, Prog. Photovoltaics 8 (2000) 171.
[5] M. Grätzel, Pure Appl. Chem. 73 (2001) 459.
[6] M. Grätzel, Nature 421 (2003) 586.
[7] U. Bach, D. Lupo, P. Comte, J.E. Moser, F. Weissortel, J. Salbeck, H. Spreitzer, M. Grätzel, Nature 395 (1998) 583.
[8] J. Kruger, R. Plass, L. Cevey, M. Piccirelli, M. Grätzel, U. Bach, Appl. Phys. Lett. 79 (2001) 2085.
[9] K. Tennakone, G.K.R. Senadeera, D.B.R.A. De Silva, I.R.M. Kottegoda, Appl. Phys. Lett. 77 (2000) 2367.
[10] K. Tennakone, G. Kumara, K.G.U. Wijayantha, I.R.M. Kottegoda, V.P.S. Perera, G. Aponsu, J. Photochem. Photobiol. A: Chem. 108 (1997) 175.
[11] A. Konno, G.R.A. Kumara, R. Hata, K. Tennakone, Electrochemistry 70 (2002) 432.
[12] G. Kumara, A. Konno, G.K.R. Senadeera, P.V.V. Jayaweera, D. De Silva, K. Tennakone, Sol. Energy Mater. Sol. Cells 69 (2001) 195.
[13] B. O'Regan, F. Lenzmann, R. Muis, J. Wienke, Chem. Mater. 14 (2002) 5023.
[14] M.K. Nazeeruddin, P. Pechy, T. Renouard, S.M. Zakeeruddin, R. Humphry-Baker, P. Comte, P. Liska, L. Cevey, E. Costa, V. Shklover, L. Spiccia, G.B. Deacon, C.A. Bignozzi, M. Grätzel, J. Am. Chem. Soc. 123 (2001) 1613.
[15] B.A. Gregg, F. Pichot, S. Ferrere, C.L.J. Fields, Phys. Chem. B (2001), ACS ASAP.
[16] S.A. Sapp, C.M. Elliott, C. Contado, S. Caramori, C.A. Bignozzi, J. Am. Chem. Soc. 124 (2002) 11215.
[17] H. Nusbaumer, J.E. Moser, S.M. Zakeeruddin, M.K. Nazeeruddin, M. Grätzel, J. Phys. Chem. B 105 (2001) 10461.
[18] H. Nusbaumer, S.M. Zakeeruddin, J.E. Moser, M. Grätzel, Chem.: Eur. J. 9 (2003) 3756.
[19] L. Kavan, M. Grätzel, Electrochim. Acta 40 (1995) 643.
[20] A.J. Bard, L.R. Faulkner, Electrochemical Methods: Fundamentals and Applications, second ed., John Wiley and Sons Inc., New York, 2001.
[21] N. Wakabayashi, F. Kitamura, T. Ohsaka, K. Tokuda, J. Electroanal. Chem. 499 (2002) 161.
[22] P.J. Cameron, L.M. Peter, J. Phys. Chem. B 107 (2003) 14394.
[23] P.J. Cameron, L.M. Peter, in preparation.